



Research paper

Cu(II)-Na(I) heterometallic coordination compounds as photocatalyst for degradation of methylene blue

Aparup Paul^a, Ennio Zangrando^b, Valerio Bertolasi^c, Subal Chandra Manna^{a,*}^a Department of Chemistry, Vidyasagar University, Midnapore 721102, West Bengal, India^b Department of Chemical and Pharmaceutical Sciences, University of Trieste, 34127 Trieste, Italy^c Dipartimento di Scienze Chimiche e Farmaceutiche, Centro di Strutturistica Diffraattometrica, Università di Ferrara, Via L. Borsari, 46, 44100 Ferrara, Italy

ARTICLE INFO

Keywords:

Cu(II)-Na(I)

Coordination polymer

Synthesis

Crystal structure, photocatalyst

ABSTRACT

Two new Cu(II)/Na(I) coordination polymers, namely, $\{[(\text{Cu}(\text{L}1)\text{Na})_2(\text{ox})(\text{ClO}_4)_2] \cdot \text{dmf}\}_n$ (**1**) and $\{[(\text{Cu}(\text{L}2)\text{Na})_2(\text{nph})] \cdot \text{H}_2\text{O}\}_n$ (**2**) were synthesized by using the Schiff base N-(2-hydroxyethoxy)ethyl-iminomethyl-phenol ($\text{H}_2\text{L}1$) with oxalate (ox) and (3-methoxy-2-hydroxybenzylidene)propanoic acid ($\text{H}_2\text{L}2$) with naphthalene-2,6-dicarboxylate anions (nph), respectively. Both the complexes were characterized using elemental analysis, FT-IR, UV-vis spectroscopic analyses. The solid state structures of complexes **1–2** were determined using single crystal X-ray crystallography that revealed for **1** the presence of dinuclear copper(II) species, $[(\text{L}1)\text{Cu}(\text{ox})\text{Cu}(\text{L}1)]$, while **2** consists of stair-like 1D $-\text{[CuL}2\text{]}_2\text{-(nph)}\text{]}_n\text{-}$ polymers. Both these fragments are further connected by Na(I) cations to form 2D supramolecular assemblies. In both the compounds the copper and sodium atoms exhibit a square pyramidal and a distorted octahedral coordination geometry, respectively. The catalytic activity of complexes **1–2** for the degradation of methylene blue (MB) was investigated under UV irradiation and in the presence of very small amount of H_2O_2 . Both the compounds were found to be photo-catalytically active, and the mechanism of photocatalysis has been discussed in detail.

1. Introduction

The design and synthesis of hetero-metallic coordination polymers (CPs) have attracted extensive research interest not only because of the intriguing structural and topological [1] novelty, but also for their remarkable potential applications in gas storage, ion exchange, nonlinear optics, chemical separation and catalysis [2–5]. In the scheming of coordination polymers, choice of ligands that affords proper donor atoms to complete the coordination sphere of the transition metal ions is of most importance [6]. Polycarboxylate ligands as multi dentate O-donors have been widely used in the construction of CPs [7]. Beside polycarboxylate linkers, multidentate flexible Schiff base ligands are frequently used to construct polynuclear complexes, as they can act as chelating, bridging and charge balance species [8]. Therefore, the use of multidentate Schiff base ligands in combination with dicarboxylate anions represents an important strategy for the synthesis of polynuclear complexes.

CPs of first series transition metals using suitable organic ligands have been reported by lots of researchers [9]. Literature survey reveals that many copper(II) containing CPs of diverse geometries display

important role in catalytic applications [10], and among these, the photo-degradation of organic dyes has received significant attention for reasons related to environmental management [11].

Most of the organic dyes are released into water from textile industries [12]. Due to their high solubility, these dyes restrict waste water treatment by usual procedures that include synthetic photo-catalysts for decomposing organic pollutants under UV-vis light [13]. Currently, commonly used photocatalytic materials with excellent performance are mainly based on TiO_2 , ZnO, metal niobate and titanate and other semiconductors with wide band gap [14]. However, these semiconductors are limited in their reducing power, resulting in the absorption of a small amount of UV light from sunlight [15]. Thus, in order to develop photo-catalysts with high efficacy and within a wide range of wavelengths in the visible region, polynuclear transition metal polymers have been synthesized. Theoretically, CPs can be very auspicious as photocatalytic degradation materials since both the ligands and metal ions can deliver the platform to produce variable band gaps, while coordinating interactions between metal and ligand can control the band gap widths [16]. Additionally, the high diversity of CPs structures permits different behaviors in photocatalytic degradation, and at the

* Corresponding author.

E-mail address: scmanna@mail.vidyasagar.ac.in (S.C. Manna).

Table 1
Crystallographic Data and Details of Refinements for Complexes 1–2.

	1	2
Empirical formula	C ₂₇ H ₃₅ Cl ₂ Cu ₂ N ₃ Na ₂ O ₁₉	C ₃₄ H ₃₀ Cu ₂ N ₂ Na ₂ O ₁₃
M	949.54	847.66
Crystal system	Orthorhombic	Triclinic
Space group	<i>P</i> ca2 ₁	<i>P</i> $\bar{1}$
<i>a</i> / Å	10.1953(2)	6.0634(5)
<i>b</i> / Å	16.4562(2)	11.8767(12)
<i>c</i> / Å	22.2449(5)	12.4577(13)
α / °	90.0	108.657(5)
β / °	90.0	92.701(6)
γ / °	90.0	103.665(6)
<i>V</i> / Å ³	3732.16(12)	818.55(14)
<i>Z</i>	4	1
Dcalc / g cm ⁻³	1.690	1.720
μ / mm ⁻¹	1.389	1.400
<i>F</i> (000)	1936	432
Reflections collected	27,420	7913
Unique reflections	9710	3035
<i>R</i> _{int}	0.0551	0.0685
Reflections <i>I</i> > 2 σ (<i>I</i>)	7949	2696
Parameters	499	245
Goodness-of-fit	1.013	1.101
<i>R</i> ₁ ^[a]	0.0446	0.0449
w <i>R</i> ₂ (<i>I</i> > 2 σ (<i>I</i>)) ^[a]	0.1077	0.1166
Residuals / e Å ⁻³	0.514, -0.797	0.312, -0.697

^[a] $R_1 = \sum |F_o| - |F_c| / \sum |F_o|$, $wR_2 = [\sum w (F_o^2 - F_c^2)^2 / \sum w (F_o^2)^2]^{1/2}$.

same time can impact the degradation efficacy [16].

Considering the above facts, in this article we report the syntheses and characterizations of two novel CPs, namely $\{[(Cu(L1)Na)_2(ox)(ClO_4)_2] \cdot dmf\}_n$ (**1**) and $\{[(Cu(L2)Na)_2(nph)] \cdot 2H_2O\}_n$ (**2**), based on Schiff base H₂L1 = N-(2-hydroxyethoxy)ethyl-iminomethyl-phenol and H₂L2 = (3-methoxy-2-hydroxybenzylidene)propanoic acid and two

dicarboxylate co-ligands (ox = oxalate and nph = naphthalene-2,6-dicarboxylate). Their UV–vis absorption, emission spectra and photocatalytic properties have been explored.

2. Experimental

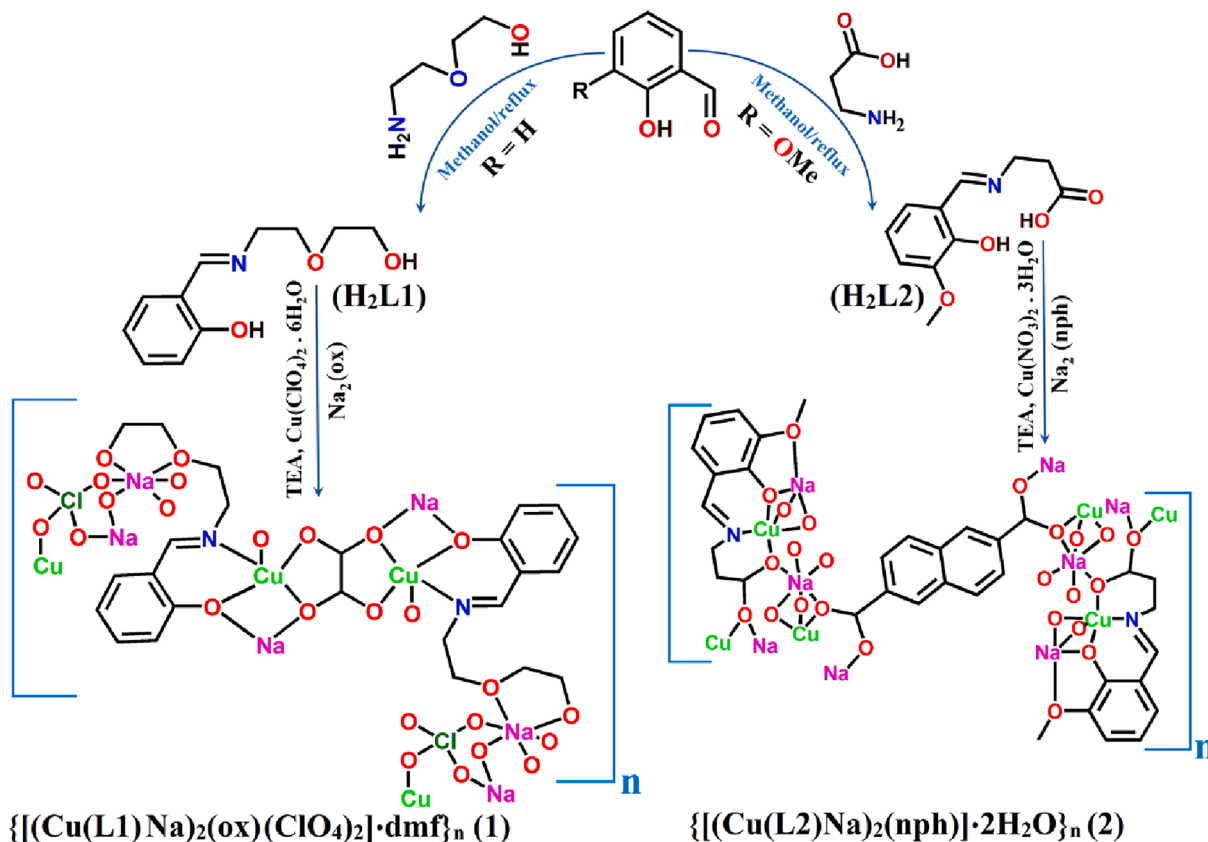
2.1. Materials and measurements

High purity 2-(2-aminoethoxy)ethanol (Aldrich), β -alanine (SRL), 2-hydroxybenzaldehyde (Spectrochem-India) and 2-hydroxy-3-methoxybenzaldehyde were purchased and used as received. All other chemicals used were of analytical grade. Solvents used for spectroscopic studies were purified and dried by standard procedures before use [17].

Elemental analyses (carbon, hydrogen and nitrogen) were performed using a Perkin-Elmer 240C elemental analyzer. IR spectra were recorded as KBr pellets on a Bruker Vector 22FT IR spectrophotometer operating from 400 to 4000 cm⁻¹. Electronic absorption spectra were obtained with Shimadzu UV-1601 UV–vis spectrophotometer at room temperature. Quartz cuvettes with a 1 cm path length and a 3 cm³ volume were used for all measurements. Emission spectra were recorded on a Hitachi F-7000 spectrofluorimeter, and room temperature (300 K) spectra were obtained using a quartz cell of 1 cm path length. The slit width was 2.5 nm for both excitation and emission. ESI-MS spectra of the compounds in water were recorded on an Agilent Q-TOF 6500 mass spectrometer and the Mass hunter software was used for mass analysis.

2.2. X-Ray crystallography

Data collections of the structures reported were carried out on a Nonius Kappa CCD diffractometer [18] equipped with graphite-monochromated Mo-K α radiation ($\lambda = 0.71073$ Å) at room temperature. Cell refinement, indexing and scaling of the data sets were carried



Scheme 1. Synthesis of ligand and complexes.

out using Denzo and Scale pack package [19]. The structures were solved by direct methods (SIR97) [20] and subsequent Fourier analyses and refined by the full-matrix least-squares method based on F^2 with all observed reflections [21]. One molecule of dimethylformamide and one of water (at half occupancy) were found in the Fourier maps of **1** and **2**, respectively. In the latter no H atoms were assigned to the slightly disordered water species. All the calculations were performed using the WinGX System, Ver 1.80.05. [22] Pertinent crystallographic data and refinement details are summarized in Table 1.

2.3. Synthesis of ligand

The ligand N-(2-hydroxyethoxy)ethyl-iminomethyl-phenol (H_2L1) was prepared by the condensation reaction of 2-(2-aminoethoxy)ethanol (2 mmol, 0.21 g) and 2-hydroxybenzaldehyde (2 mmol, 0.244 g) in methanol (20 mL), refluxing the solution for 3 h, whereas (3-methoxy-2-hydroxybenzylidene)propanoic acid (H_2L2) was prepared by the condensation reaction of β -alanine (2 mmol, 0.178 g) and 2-hydroxy-3-methoxybenzaldehyde (2 mmol, 0.304 g) in water : methanol (1:9, 20 mL), following the same procedure as for H_2L1 (Scheme 1). The yellow colored methanolic solutions were used directly for the synthesis of complexes.

2.4. Synthesis of complexes

Caution! Perchlorate salts of metal with organic ligands are potentially explosive. Only a small amount of material should be prepared, and it should be handled with care.

The complexes have been synthesized by adopting the procedures schematically given in Scheme 1.

2.4.1. Synthesis of $\{[(Cu(L1)Na)_2(ox)(ClO_4)_2] \cdot dmf\}_n$ (**1**)

Methanolic solution (5 mL) of triethylamine (1 mmol, 0.101 g) was added drop wise to a methanolic solution (10 mL) of H_2L1 (1 mmol, 10 mL) under stirring condition for 10 min. To the resulting mixture, drop wise addition of methanolic solution (15 mL) of copper perchlorate hexahydrate (1 mmol; 0.370 g) yielded a deep green solution. To this solution an aqueous solution of disodium oxalate (0.5 mmol, 0.067 g) was added after 1 h and additionally stirred for 1 h and filtered. The filtrate was kept in open atmosphere for slow evaporation obtaining after a few days a green crystalline material, not suitable for X-ray structural analysis. The green compound was dissolved in dmf and recrystallized to provide suitable crystals for X-ray diffraction. Yield: 72 %. $C_{27}H_{35}Cl_2Cu_2N_3Na_2O_{19}$ (949.54): C, 34.15; H, 3.72; N, 4.43 (%). Found: C, 34.37; H, 3.69; N, 4.38 (%). IR (cm^{-1}): 3573 (s, br), 3420 (s, br), 2922 (vw), 1662 (vs), 1621 (vs), 1595(s), 1543 (s), 1473 (w), 1446 (s), 1348 (w), 1317 (s), 1242 (vw), 1200 (vw) 1081 (vs), 898 (w), 760 (w), 662 (vw).

2.4.2. Synthesis of $\{[(Cu(L2)Na)_2(nph)] \cdot H_2O\}_n$ (**2**)

Methanolic solution (5 mL) of triethylamine (1 mmol, 0.101 g) was added dropwise to a methanol : water (9:1) solution of H_2L2 (1 mmol, 10 mL) in stirring condition for 10 min. To this resulting mixture, methanolic solution (10 mL) of copper nitrate trihydrate (1 mmol; 0.241 g) was added and left for stirring for 30 min. A deep green solution was obtained. After that an aqueous solution of disodium naphthalene-2,6-dicarboxylate (0.5 mmol, 0.13 g) was added and transferred the resulting solution to a Teflon lined stainless steel reactor and heated to 80 °C for six hours, followed by cooling slowly to room temperature. After 18 h the solution was filtered and the filtrate was kept in open atmosphere for slow evaporation and green color single crystal suitable for X-ray diffraction was obtained after a few days. Yield: 77 %. $C_{34}H_{30}Cu_2N_2Na_2O_{13}$ (847.66): C, 48.17; H, 3.57; N, 3.30 (%). Found: C, 48.11; H, 3.61; N, 3.32 (%). IR (cm^{-1}): 3596 (w, br), 3417 (w, br), 2912 (w), 1605 (vs), 1473 (vs), 1448(s), 1367 (vs), 1325 (vs), 1238 (s), 1216 (vs), 1190 (w), 1074 (s), 1039 (w) 961 (vs), 862 (s), 780 (vs), 743 (vs),

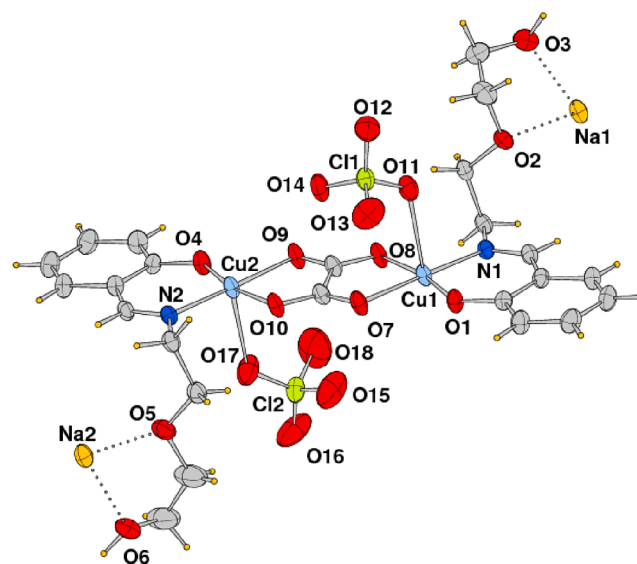


Fig. 1. Dinuclear copper complex **1** (ellipsoid probability at 35%; C atoms not labelled for sake of clarity; dmf molecule not shown).

633 (vw), 605 (vw).

2.5. Photocatalytic experiment

The photocatalytic performance of **1** and **2** was investigated for the degradation of methylene blue (MB) in a typical process. A crystalline sample (5 mg) of each complex was mixed with 100 mL of MB aqueous solution (1 mg litre^{-1}). The mixture was stirred for 30 min in a dark environment. After that 50 μL of H_2O_2 30% were added to the solution and stirred continuously under UV irradiation of a 125 W mercury lamp at a distance of 4–5 cm from the liquid surface. At intervals of 30 min, 3 mL of the sample were taken from the container and analyzed by UV–vis spectroscopy. The MB concentration changes were monitored by measuring the absorbance intensity at its characteristic absorbance wavelength of $\lambda = 664 \text{ nm}$. The experimental data were analyzed by a first order kinetic model. The degradation rate and the kinetic rate constant (k) were calculated [23] using the equations:

$$\text{Degradation (\%)} = (1 - A/A_0) \times 100 \text{ and } -\ln(C/C_0) = k \times t$$

where A and A_0 are the absorbance at time t and $t = 0$, respectively, corresponding to the relative concentrations C and C_0 .

2.6. Band-gap calculations

The band gap of complexes was examined by the UV–vis diffuse reflection measurement process at room temperature, and the band-gap energy evaluated from the Tauc plot $(\alpha h\nu)^2$ versus photon energy ($h\nu$) for a particular sample according to equation.

$$(\alpha h\nu) = K(h\nu - E_g)^n$$

where α is the absorption co-efficient, $h\nu$ is the discrete photon energy, K is a constant which is considered as 1 for ideal case, and E_g is the band gap energy [13]. To determine the direct band gap, the value of the exponent 'n' in the above equation has been considered equal to 1/2 [13b]. The extrapolated value along the X axis of $h\nu$ at $\alpha = 0$ gives the absorption edge energies corresponding to E_g [23c–23d]. The point of inflection in the Tauc plot gives the particular value of the band-gap energy.

Table 2
Selected bond distances (Å) and angles (°) for complex 1.

Cu(1)-O(1)	1.874(4)	Cu(2)-O(4)	1.872(4)
Cu(1)-N(1)	1.943(4)	Cu(2)-N(2)	1.941(4)
Cu(1)-O(7)	2.002(3)	Cu(2)-O(9)	2.019(3)
Cu(1)-O(8)	1.984(4)	Cu(2)-O(10)	1.991(4)
Cu(1)-O(11) ^d	2.540(4)	Cu(2)-O(17) ^c	2.534(6)
Na(1)-O(2)	2.502(4)	Na(2)-O(1) ^c	2.414(4)
Na(1)-O(3)	2.342(5)	Na(2)-O(5)	2.529(4)
Na(1)-O(4) ^d	2.378(4)	Na(2)-O(6)	2.323(6)
Na(1)-O(9) ^d	2.364(4)	Na(2)-O(7) ^c	2.384(4)
Na(1)-O(12)	2.486(6)	Na(2)-O(13) ^a	2.520(6)
Na(1)-O(18) ^b	2.580(11)	Na(2)-O(16)	2.394(7)
O(1)-Cu(1)-O(7)	85.91(14)	O(4)-Cu(2)-O(9)	85.03(15)
O(1)-Cu(1)-O(8)	168.52(14)	O(4)-Cu(2)-O(10)	167.73(13)
O(1)-Cu(1)-N(1)	96.56(16)	O(4)-Cu(2)-N(2)	96.10(17)
O(1)-Cu(1)-O(11) ^d	93.46(12)	O(4)-Cu(2)-O(17) ^c	87.93(14)
O(7)-Cu(1)-O(8)	82.72(14)	O(9)-Cu(2)-O(10)	82.82(14)
O(7)-Cu(1)-N(1)	176.59(16)	O(9)-Cu(2)-N(2)	177.35(18)
O(7)-Cu(1)-O(11) ^d	92.29(11)	O(9)-Cu(2)-O(17) ^c	92.17(14)
O(8)-Cu(1)-N(1)	94.74(16)	O(10)-Cu(2)-N(2)	95.97(16)
O(8)-Cu(1)-O(11) ^d	88.57(12)	O(10)-Cu(2)-O(17) ^c	94.27(13)
N(1)-Cu(1)-O(11) ^d	89.91(11)	N(2)-Cu(2)-O(17) ^c	90.27(15)
O(2)-Na(1)-O(4) ^d	153.70(17)	O(5)-Na(2)-O(1) ^c	156.46(18)
O(3)-Na(1)-O(18) ^b	157.5(3)	O(6)-Na(2)-O(13) ^a	169.6(2)
O(12)-Na(1)-O(9) ^d	175.65(19)	O(16)-Na(2)-O(7) ^c	171.7(2)

Symmetry codes: a = x, -1+y, z; b = x, 1+y, z; c = 1/2+x, -y, z; d = -1/2+x, 1-y, z.

3. Results and discussion

3.1. Synthetic aspect

The Schiff base ligands, N-(2-hydroxyethoxy)ethyl-iminomethylphenol (H₂L1) and (3-methoxy-2-hydroxybenzylidene) propanoic acid (H₂L2) were synthesized by adopting the condensation reaction between corresponding amine and aldehyde in methanol under reflux condition. Then H₂L1 and H₂L2 were used for the synthesis of complexes 1 and 2.

3.2. Crystal structure description of $\{[(Cu(L1)Na)_2(ClO_4)_2(ox)] \cdot dmf\}_n$ (1)

The X-ray structural analysis reveals that the asymmetric unit of compound 1 comprises a dinuclear Cu(II) complex, two perchlorate anions, two sodium ions (Fig. 1) and a lattice dmf molecule. In the complex each copper atom is chelated by a Schiff base through the imino N and the phenolate O atoms and these fragments are further connected by an oxalate anion in a bis-bidentate fashion with metals separated by 5.235(1) Å.

The copper atoms exhibit a square pyramidal geometry completing their coordination sphere by a perchlorate anion at apical position. The Cu–O(phenol) bond distances are of 1.874(4), 1.872(4) Å, while the Cu–O(oxalate) ones are slightly different, being of 1.984(4) and 1.991(4) Å those in trans to the phenol oxygen, and of 2.002(3) and 2.019(3) Å those trans located to the imino nitrogen (Table 2). Finally the Cu–N bond distances are of 1.943(4) and 1.941(4) Å, while the Cu–O ones of

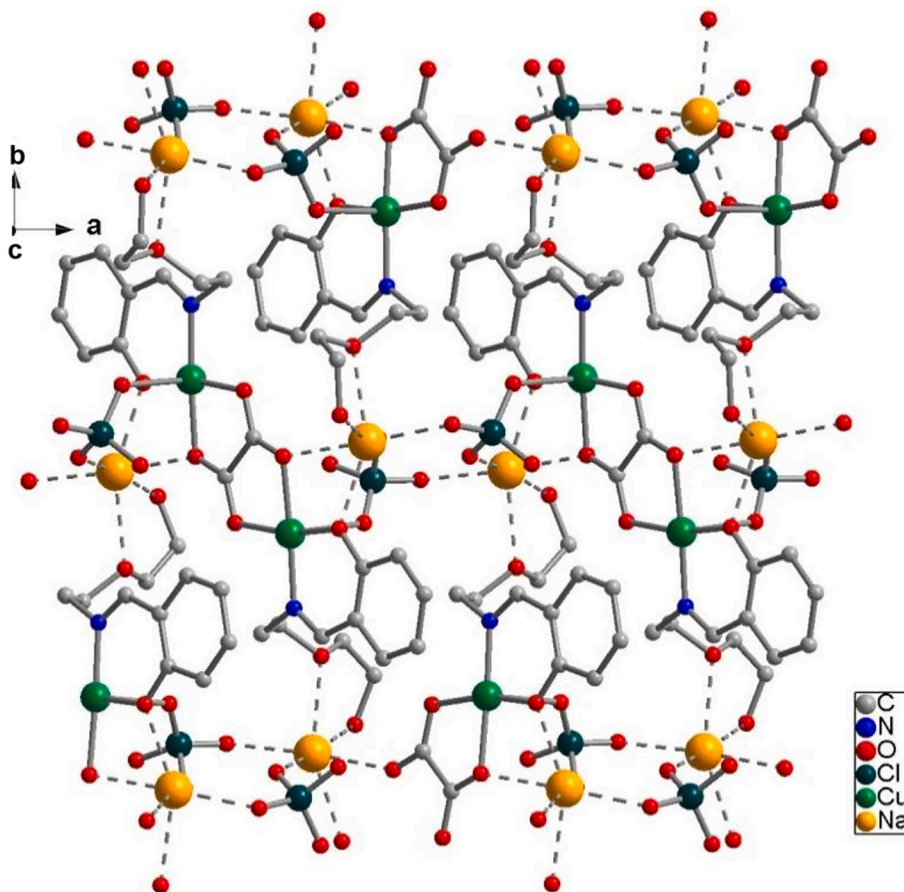


Fig. 2. The 2D polymer of compound 1 (Na–O bonds are indicated as dotted lines; lattice dmf molecules not shown).

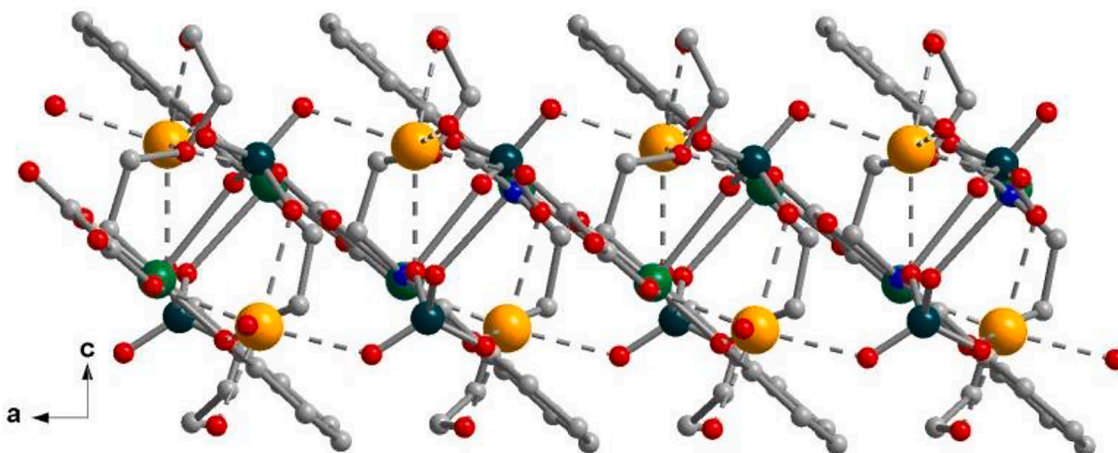


Fig. 3. 2D polymer of compound 1 viewed down axis *b*.

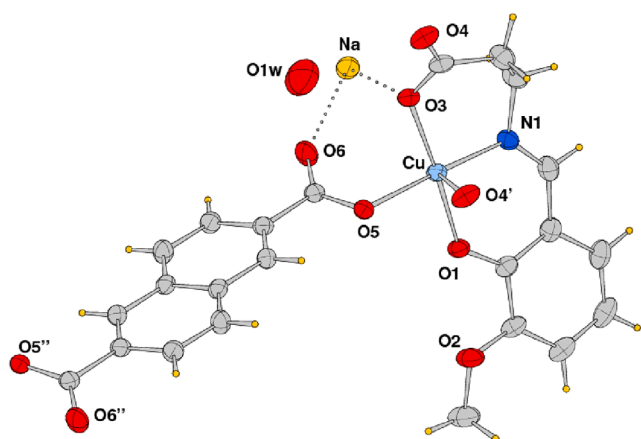


Fig. 4. The asymmetric unit (Ortep drawing, 30% ellipsoid probability) of compound 2 with the naphthalene-dicarboxylate species located on a center of symmetry (O4' at 1-*x*, -*y*, 1-*z*; O5'/O6'' at 1-*x*, -1-*y*, -*z*).

apical perchlorate ligand present the longest values, of 2.540(4) and 2.534(6) Å. The dinuclear entity shows an almost centro-symmetrical fashion, the main difference being exhibited by a different conformation of the (2-hydroxyethoxy)ethyl chains that pend hedge-wise. The copper complexes are connected by sodium cations to form a 2D supramolecular assembly parallel to the crystallographic *ab* plane (Fig. 2).

In fact both the sodium ions, embedded among the complexes, result coordinated by the oxygen atoms of one (2-hydroxyethoxy)ethyl arm and in addition chelated by the oxalate and phenol oxygen atoms of a symmetry related complex and finally bound by two oxygen atoms of perchlorate anions, giving rise to a highly distorted octahedral geometry (Figs. 2 and 3).

The Na-O bond lengths fall in a range from 2.323(6) to 2.580(11) Å (Table 2), in agreement with values measured in other copper(II)/sodium(I) compounds [24]. The O-Na-O coordination bond angle values of trans located O oxygen atoms (Table 2) indicate the deviations from the ideal octahedral values. Thus the perchlorate anions act as bridging units between the sodium and copper atoms which are separated by 3.279(2) Å (Na(1)...Cu(2) at $-1/2 + x, 1-y, z$) and 3.340(2) Å (Na(2)...Cu(1) at $1/2 + x, -y, z$). Both alcoholic groups O3 and O6 (from different

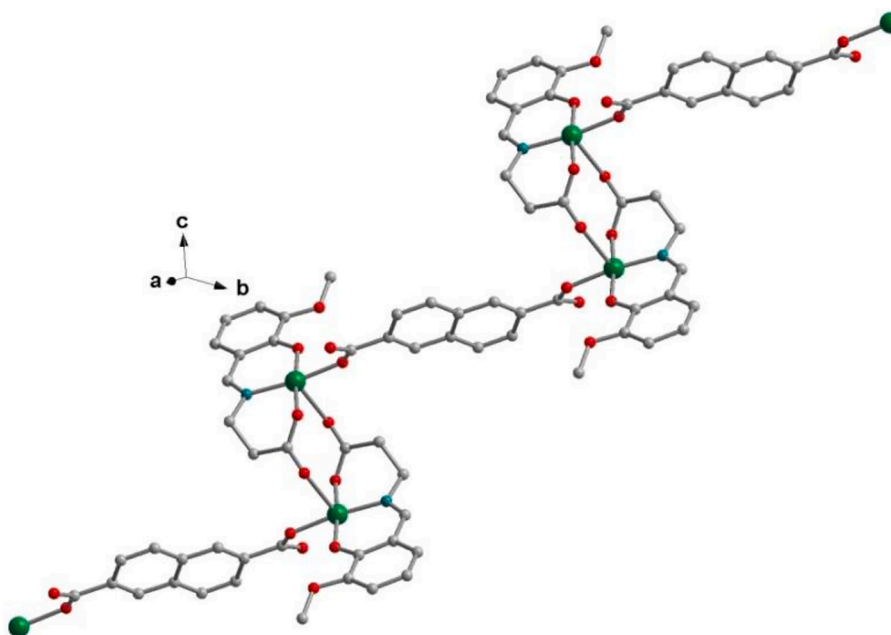


Fig. 5. The 1D chain built by the (CuL2)₂ centrosymmetric dimers connected by the nph anions.

Table 3
Selected bond distances (Å) and angles (°) for complex 2.

Cu–O(1)	1.897(2)	Na–O(2)a	2.699(3)
Cu–O(3)	1.951(2)	Na–O(3)	2.430(3)
Cu–N(1)	1.952(3)	Na–O(4)c	2.735(3)
Cu–O(5)	1.967(2)	Na–O(5)a	2.457(3)
Cu–O(4)e	2.441(3)	Na–O(6)	2.271(3)
Na–O(1)a	2.274(3)	Na–Cu _a	3.1462(14)
O(1)–Cu–O(3)	174.66(10)	O(3)–Cu–N(1)	92.60(11)
O(1)–Cu–O(5)	83.64(10)	O(3)–Cu–O(4)e	90.53(10)
O(1)–Cu–N(1)	92.45(11)	O(5)–Cu–N(1)	173.18(11)
O(1)–Cu–O(4)e	86.83(10)	O(5)–Cu–O(4)e	84.43(11)
O(3)–Cu–O(5)	91.50(10)	N(1)–Cu–O(4)e	100.98(12)
O(3)–Na–O(6)	79.73(10)	O(6)–Na–O(5)a	124.49(11)
O(3)–Na–O(1)a	117.92(11)	O(6)–Na–O(4)c	145.39(12)
O(3)–Na–O(2)a	96.10(11)	O(1)a–Na–O(2)a	61.34(9)
O(3)–Na–O(5)a	140.04(11)	O(1)a–Na–O(5)a	65.86(9)
O(3)–Na–O(4)c	73.68(9)	O(1)a–Na–O(4)c	73.12(9)
O(6)–Na–O(1)a	140.43(13)	O(2)a–Na–O(5)a	116.47(11)
O(6)–Na–O(2)a	82.81(11)	O(2)a–Na–O(4)c	121.29(10)
		O(5)a–Na–O(4)c	69.87(9)

Symmetry codes: a = -1 + x, y, z; b = 1 + x, y, z; c = -x, -y, 1-z; d = 1-x, 1-y, -z; e = 1-x, -y, 1-z.

complexes) interacts with the dmf oxygen through H-bond interactions (O...O distances of 2.788(8) Å).

3.3. Crystal structure description of $\{[(\text{Cu}(\text{L}2)\text{Na})_2(\text{nph})] \cdot \text{H}_2\text{O}\}_n$ (2)

The asymmetric unit of compound 2, shown in Fig. 4, consists of a CuL2 unit, half naphthalene-2,6-dicarboxylate anion, a sodium ion, and a residual interpreted as half lattice water molecule. For the latter, hydrogen atoms were not located. The crystal packing comprises of $[\text{CuL}2]_2$ dimers further connected by the naphthalene-2,6-dicarboxylate anions to form a stair-like 1D polymeric arrangement (Fig. 5).

The copper atom exhibits a square pyramidal geometry being chelated by the Schiff base through the phenolato oxygen (Cu–O(1) = 1.897(2) Å), the imino nitrogen (Cu–N(1) = 1.952(3) Å), and a carboxylate oxygen of the propanoate chain (Cu–O(3) = 1.951(2) Å), completing the basal plane with an oxygen of the naphthalene-2,6-dicarboxylate anion (Cu–O(5) = 1.967(2) Å). Two of these fragments are arranged about a crystallographic center of symmetry in such a way that one propanoate oxygen of each complex coordinates the metal of the other at apical position (Cu–O(4)' = 2.441(3) Å, O(4)' at 1-x, -y, 1-z). The copper atom is slightly displaced by 0.03 Å from the best-fit NO_3 plane towards the apical oxygen donor.

The sodium cation presents a six-coordination in a distorted trigonal prismatic molecular geometry with Na–O distances in a wide range from 2.271(3) to 2.735(3) Å, involving oxygen atoms O(1–6) from three symmetry related copper complexes. The O–Na–O coordination bond angles reported in Table 3 are indicative of the highly distorted octahedral geometry. Fig. 6 shows the NaO_6 polyhedra connecting the polymeric chains of Fig. 5 to form a 2D architecture parallel to the bc plane. No short phenyl ring interaction with centroid-to-centroid distance shorter than 4.5 Å is detected in the crystal packing.

3.4. Electronic absorption and emission spectra of complexes

The electronic spectra of complexes 1 and 2 were recorded in water. The spectrum of 1 (Fig. S1) shows significant transitions at 215 nm ($\epsilon \sim 1.65 \times 10^5 \text{ M}^{-1} \text{ cm}^{-1}$), 235 nm ($\epsilon \sim 1.36 \times 10^5 \text{ M}^{-1} \text{ cm}^{-1}$), 266 nm ($\epsilon \sim 9.26 \times 10^4 \text{ M}^{-1} \text{ cm}^{-1}$) and 354 nm ($\epsilon \sim 2.84 \times 10^4 \text{ M}^{-1} \text{ cm}^{-1}$). Conversely, the absorption spectrum of 2 (Fig. S1) exhibits significant transitions at 237 nm ($\epsilon \sim 1.63 \times 10^5 \text{ M}^{-1} \text{ cm}^{-1}$), 273 nm ($\epsilon \sim 4.98 \times 10^4 \text{ M}^{-1} \text{ cm}^{-1}$) and 364 nm ($\epsilon \sim 1.12 \times 10^4 \text{ M}^{-1} \text{ cm}^{-1}$). Both the complexes display red shifted emission. On excitation at 354 nm complex 1 displays luminescence bands at 407 and 498 nm (Fig. S2),

whereas complex 2 exhibits bands at 361 and 404 nm upon excitation at 273 nm (Fig. S3). The positions of emission bands remain unaffected when λ_{ex} is varied within ± 10 nm.

3.5. ESI mass spectrometry

ESI mass spectra of complexes were recorded in water. The ESI mass spectrum of 1 (Fig. S4) shows a peak at $m/z = 876.0177$, corresponding to $[\text{C}_{24}\text{H}_{28}\text{Cl}_2\text{Cu}_2\text{N}_2\text{Na}_2\text{O}_{18}]^+$ (calc. $m/z = 876.46$). Alternatively the spectrum of 2 (Fig. S5) shows a peak at $m/z = 847.0412$, corresponding to $[\text{C}_{34}\text{H}_{30}\text{Cu}_2\text{N}_2\text{Na}_2\text{O}_{13}]^+$ (calc. $m/z = 847.68$). These results evidences that the species of 1 and 2 in water are composed of dinuclear copper fragments (bound to two Na cations), a structure formally similar to the building units forming the polymers detected in solid state.

3.6. Band-gap studies

The difference in the band-gap sizes influences the photo-catalytic activity of coordination polymers. For this reason, we were motivated to estimate the band-gap value of complexes at room temperature using the UV–vis diffuse reflectance measurement method. The calculated values of band gap (Fig. S6) of 1 and 2 are 2.87 ± 0.03 and 3.01 ± 0.06 eV, respectively, indicating that these materials are semiconductors in nature. These results give emphasis to the relative strength of complexes for photocatalytic applications. In the complexes with lower degree of electronic band-gap, charge transfer from 2p bonding orbitals (valence band) of oxygen and nitrogen to empty orbital (conduction band) of copper takes place easily, thus favouring photo-catalytic activity [23b].

3.7. Photocatalytic activity

Methylene blue (MB), a chemically stable and poor biodegradable species, typically difficult to decompose in waste water [25], was selected for evaluating the photocatalytic properties of complexes 1 and 2 toward the decomposition of organic pollutants. We are aware that polymeric complexes 1 and 2 are dissociated in solution to form simpler species, and in fact ESI mass spectra in water indicate complex fragments as the building blocks forming the polymers observed in solid state. With this premise, Fig. 7 illustrates the time dependent electronic absorption spectra of the MB solution degraded by the complexes, by monitoring the process of photo degradation at the characteristic absorption of MB at 664 nm. The spectra of Fig. 7 clearly demonstrate that the absorption peak of MB gradually decreased with irradiation time in presence of the metal complexes. The fading of color could be simply detected by naked eye in the photocatalytic process (inset of Fig. 7). The plot of Fig. 8 shows the variation of C/C₀ against irradiation time (where C₀ is the initial concentration of MB and C is the apparent concentration at different intervals of time).

The degradation rate estimates that about 63% of MB degradation occurred after 150 min in presence of complex 1 under UV irradiation, and 61% for complex 2. Some parallel experiments were conducted on the degradation of dye solution under the following reaction conditions:

(i) in presence of H_2O_2 in the dark (Fig. S7); (ii) in presence of H_2O_2 and light irradiation (Fig. S7); (iii) in presence of complexes and light irradiation in the absence of H_2O_2 (Fig. S8); (iv) in presence of isopropyl alcohol, H_2O_2 and light irradiation (Fig. S9). Experimental results show that after 150 min tiny degradation of MB can be detected in presence of H_2O_2 in the dark. The degradation rate under Hg lamp is 30% with H_2O_2 only, and 27 and 22% in the presence of only complexes 1 and 2, respectively, but these values increase to 63 and 61% upon addition of H_2O_2 (Fig. 8) under UV light irradiation. Photocatalytic activities of the solutions of mixtures of (i) $\text{Cu}(\text{ClO}_4)_2 \cdot 6\text{H}_2\text{O}$ and $\text{H}_2\text{L}1$ (1:1), and (ii) $\text{Cu}(\text{NO}_3)_2 \cdot 3\text{H}_2\text{O}$ and $\text{H}_2\text{L}2$ (1:1) have also been investigated under same experimental conditions to compare with the catalytic activities with complexes 1 and 2. Experimental results show that (Fig. S10) after 150 min very small amount of MB degradation were detected (11% for the

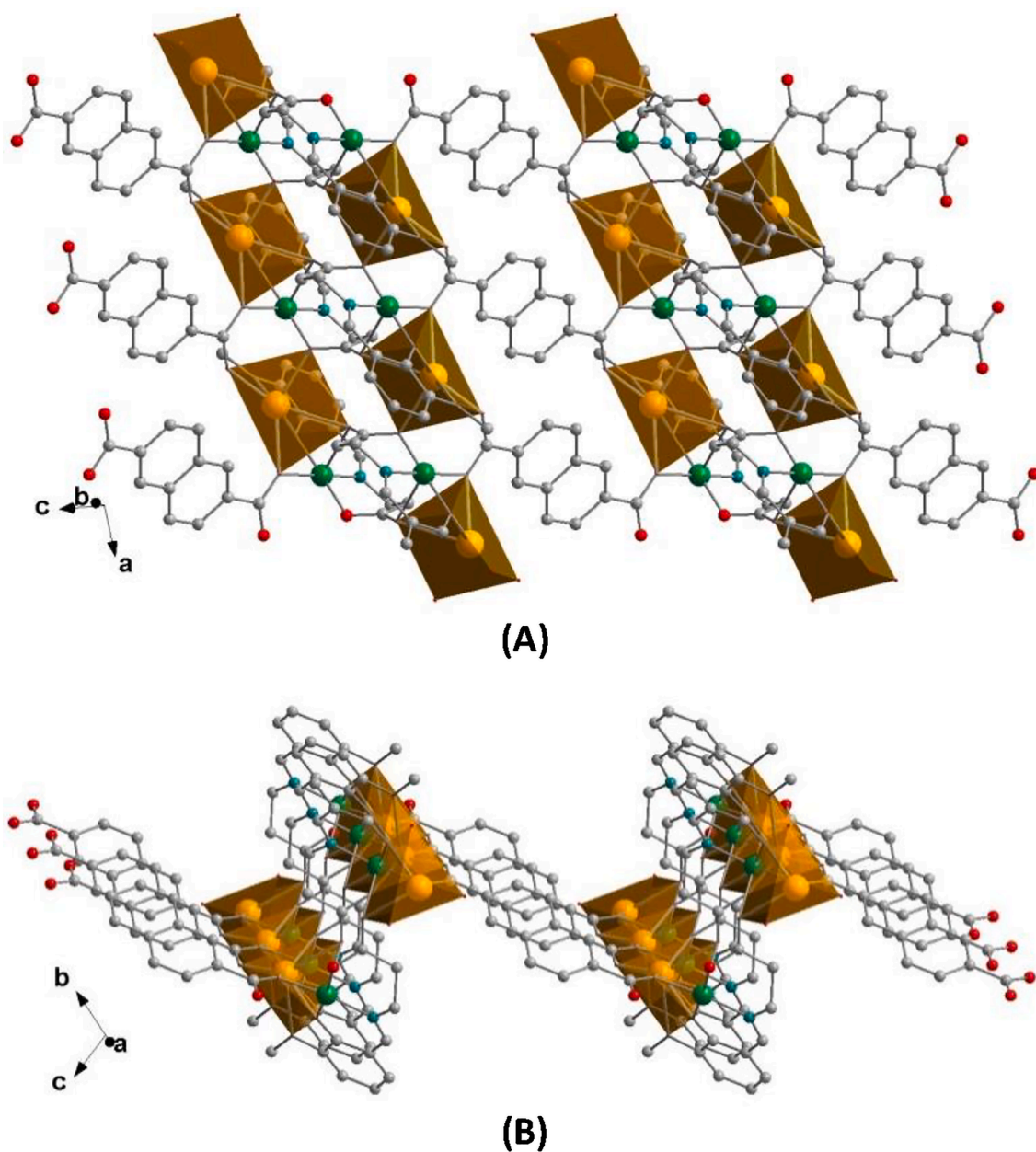


Fig. 6. (A) The 2D architecture built by NaO_6 polyhedra; (B) perspective view of the 2D supramolecular structure.

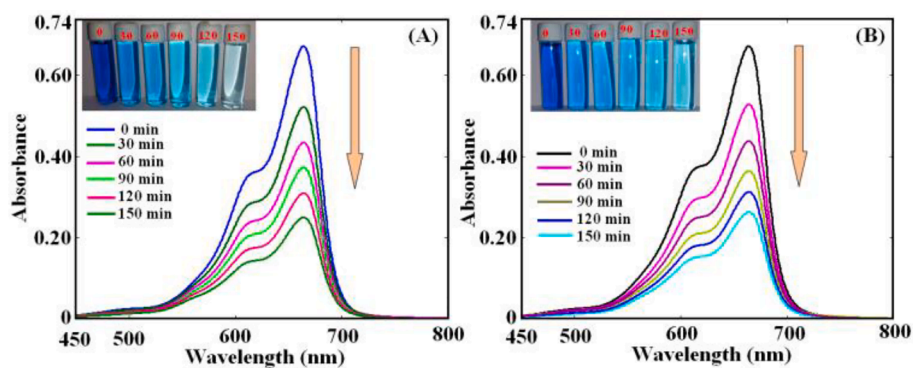


Fig. 7. Change in the UV-vis spectra of the degradation of MB in the presence of complex 1 (A) and 2 (B) under UV irradiation. Inset: Color change photograph of MB solutions in the presence of complexes taken at intervals of 30 min.

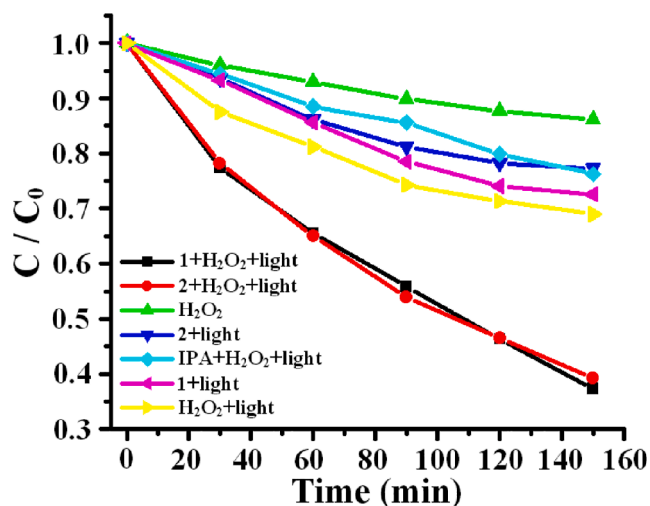


Fig. 8. The MB degradation with different photocatalytic conditions.

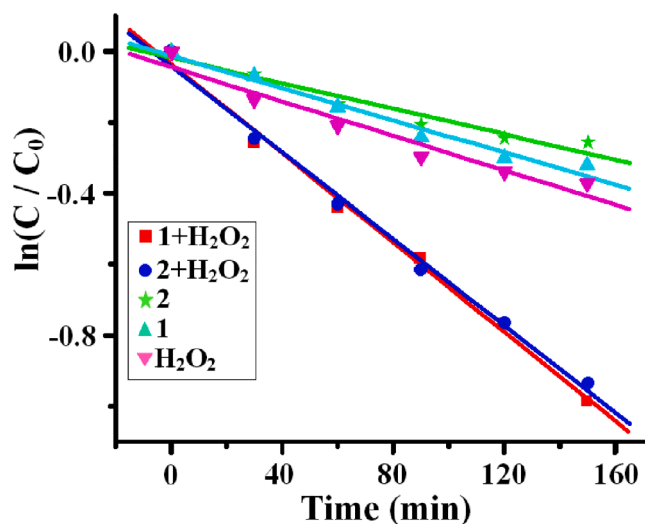


Fig. 9. The reaction kinetics of MB over the two complexes at different conditions.

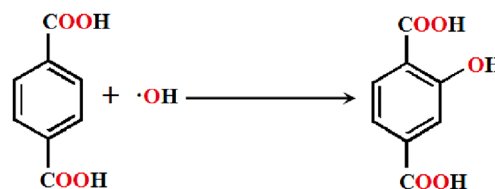
solution of $\text{Cu}(\text{ClO}_4)_2 \cdot 6\text{H}_2\text{O}$ and $\text{H}_2\text{L1}$; 14% for the solution of $\text{Cu}(\text{NO}_3)_2 \cdot 3\text{H}_2\text{O}$ and $\text{H}_2\text{L2}$. All the above results reveal that the presence of the metal complex is essential for effective degradation of the organic dye MB, and both the complexes show high photocatalytic activity.

3.8. Kinetics of the catalytic photodegradation reaction

In order to obtain a better understanding of the reaction kinetics of the MB degradation catalyzed by the complexes, the experimental data were fitted by Langmuir-Hinshelwood model (a first-order kinetic model). The value of the rate constant (k) usually provides an indication of the photocatalytic activity of the complexes. Fig. 9 shows the linear relationship between $\ln(C/C_0)$ against the irradiation time for MB degradation under conditions indicated.

The rate constants of 1 and 2 for the photodegradation of MB in presence of H_2O_2 are 0.00629 and 0.00611 min^{-1} , respectively. The result showed that addition of hydrogen peroxide electron acceptor can easily increase the photo-catalytic activities. The synergy index (SI) was calculated using the following equation: [23b].

$$\text{SI} = \frac{k_{(\text{H}_2\text{O}_2+1/2)}}{k_{\text{H}_2\text{O}_2} + k_{1/2}}$$



Scheme 2. Formation of 2-hydroxy terephthalic acid in the presence of hydroxyl radicals.

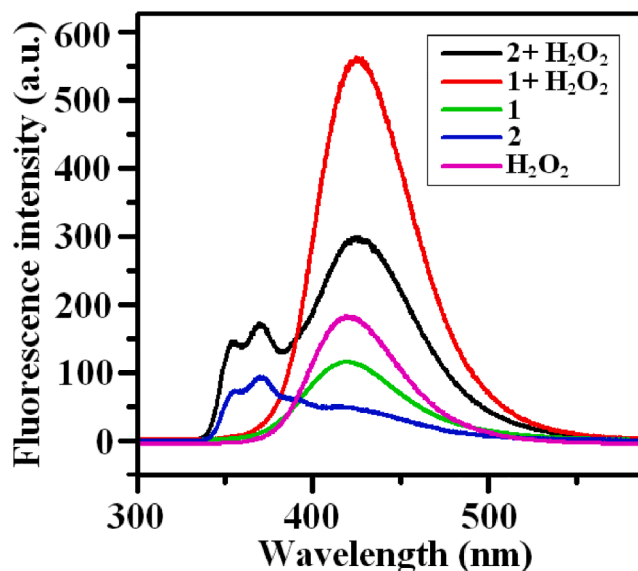


Fig. 10. The emission spectra of TAOH formed by the reaction of TA with hydroxyl radicals generated from different photocatalytic system under UV light for 30 min.

Where $k_{(\text{H}_2\text{O}_2+1/2)}$ is the rate constant of the complex in presence of H_2O_2 under irradiation, $k_{\text{H}_2\text{O}_2}$ is the rate constant in presence of H_2O_2 under irradiation without any catalyst, and $k_{1/2}$ is the rate constant in presence of complex 1 (or 2) under irradiation without H_2O_2 . The calculated SI values are 1.338 and 1.444 for complex 1 and 2, respectively, which can describe the degree of synergy with the electron acceptor.

3.9. Reaction mechanism of photocatalytic degradation of methylene blue

The reaction mechanism for the degradation of MB may proceed via two possible pathways: (i) a catalytically promoted decomposition by the Cu(II) complexes to produce hydroxyl radicals ($\cdot\text{OH}$) through a Fenton-like reaction, where Cu(II) reacts through a Cu(II)-Cu(I) redox cycle; [26] (ii) by absorption of energy \geq the band gap of the Cu(II) complexes and consequent electron promotion from the valence band (VB) to the conduction band (CB), leaving holes (h^+) in the valence band (eq. (1)). The electrons reduce O_2 to $\cdot\text{O}_2$ and finally produce hydroxyl radicals ($\cdot\text{OH}$) (eq. (3)). On the other hand photoexcited holes have strong oxidant ability and can oxidize hydroxyl ions (OH^-) or adsorb organic molecules to $\cdot\text{OH}$ (eq. (2)). H_2O_2 is an electron acceptor which provides more $\cdot\text{OH}$ by accepting electrons from CB within the photocatalytic system (eq. (4)). The formed radical $\cdot\text{OH}$ possesses the ability to effectively decompose methylene blue [27].





To explore the role of the reactive species during the photo-degradation of methylene blue we carried out trapping experiment with terephthalic acid (TA) in basic solution using fluorescence spectroscopy technique [28]. In basic solution TA reacts with $\cdot OH$ to generate 2-hydroxyterephthalic acid (TAOH), which emits at 426 nm (Scheme 2).

Upon 30 min irradiation of TA (0.5 mM in KOH solution) in the presence of only H_2O_2 , **1** and **2**, the fluorescence intensities are 179, 117 and 48, respectively (Fig. 10). However adding complexes and H_2O_2 together the fluorescence intensity of the TAOH peak reaches a value of 561 (for **1**) and 297 (for **2**). This finding clearly indicates that the addition of H_2O_2 in the photocatalytic system produced more $\cdot OH$ radicals and degrade MB effectively.

The role of $\cdot OH$ in degradation of MB was further explored by radical trapping experiments for complex **1**. 1 mM isopropyl alcohol (IPA) was added to the mixture solution and the degradation experiment was carried out under same conditions as stated in the experimental section. A significant inhibition was observed in the degradation of methylene blue by the addition of IPA as $\cdot OH$ scavenger compared with the lack of scavenger under same reaction conditions (Fig. 8 and Fig. S9). From the above trapping experiments, it can be concluded that $\cdot OH$ radical becomes the main reactive species in the whole photodegradation process of MB in presence of complexes and H_2O_2 under UV irradiation.

4. Conclusions

In summary, we have successfully synthesized two new Cu(II)/Na(I) coordination polymers constructed from two Schiff bases (N-(2-hydroxyethoxy)ethyl-iminomethyl-phenol and (3-methoxy-2-hydroxybenzylidene)propanoate) and two dicarboxylate ligands (oxalate and naphthalene-2,6-dicarboxylate). The X-ray structural analysis reveals that both dinuclear copper species, which are connected by Na(I) ions, form a 2D supramolecular assembly, and a stair-like 1D polymeric arrangement, respectively. Photocatalytic experiments demonstrate that both the compounds can efficiently degrade methylene blue under UV light irradiation in presence of small amount of H_2O_2 , and the reaction mechanism indicated that radical $\cdot OH$ appears the main reactive species in the whole process.

CRediT authorship contribution statement

Aparup Paul: Conceptualization, Formal analysis, Investigation, Methodology, Project administration, Visualization, Writing - original draft. **Ennio Zangrando:** Formal analysis, Software, Validation, Visualization, Writing - review & editing. **Valerio Bertolasi:** Formal analysis, Software. **Subal Chandra Manna:** Conceptualization, Funding acquisition, Project administration, Resources, Supervision, Writing - review & editing.

Declaration of Competing Interest

The authors declare that they have no known competing financial interests or personal relationships that could have appeared to influence the work reported in this paper.

Acknowledgements

The authors gratefully acknowledge the financial assistance given by the CSIR, Government of India, to Dr. Subal Chandra Manna (Project No. 01 (2743)/13/EMR-II).

Appendix A. Supplementary data

Supplementary data to this article can be found online at <https://doi.org/10.1016/j.ica.2021.120346>.

References

- Y. Tezuka, H. Oike, *J. Am. Chem. Soc.* 123 (2001) 11570–11576;
 - K. Kasai, M. Aoyagi, M. Fujita, *J. Am. Chem. Soc.* 122 (2000) 2140–2141;
 - D. Kumar, A. Das, P. Dastidar, *Inorg. Chem.* 46 (2007) 7351–7361;
 - C. Livage, P. Forster, N. Guillou, M. Tafoya, A. Cheetham, G. Férey, *Angew. Chem. Int. Ed.* 119 (2007) 5981–5983.
- Y.P. He, Y.X. Tan, F. Wang, J. Zhang, *Inorg. Chem.* 51 (2012) 1995–1997;
 - W.Y. Gao, W.M. Yan, R. Cai, K. Williams, A. Salas, L. Wojtas, X.D. Shi, S.Q. Ma, *Chem. Commun.* 48 (2012) 8898–8900.
- X. Zhang, Z.J. Wang, S.G. Chen, Z.Z. Shi, J.X. Chen, H.G. Zheng, *Dalton Trans.* 46 (2017) 2332–2338;
 - C.L. Zhang, L. Qin, Z.Z. Shi, H.G. Zheng, *Dalton Trans.* 44 (2015) 4238–4245;
 - L.L. Liu, C.X. Yu, J.M. Du, S.M. Liu, S.N. Wang, S.J. Lin, X.Y. Li, D. Sun, *Dalton Trans.* 44 (2015) 11013–11020;
 - L.L. Han, T.P. Hu, K. Mei, C. Yin, Y.X. Wang, J. Zheng, X.P. Wang, D. Sun, *Dalton Trans.* 44 (2015) 6052–6061.
- J. Yang, J.F. Ma, S.R. Batten, *Chem. Commun.* 48 (2012) 7899–7912;
 - M. Yadav, A. Bhunia, S.K. Jana, P.W. Roesky, *Inorg. Chem.* 55 (2016) 2701–2708;
 - A.M. Spokoiny, D. Kim, A. Sumrein, C.A. Mirkin, *Chem. Soc. Rev.* 38 (2009) 1218–1227;
 - W.H. Zhu, S. Li, C. Gao, X. Xiong, Y. Zhang, L. Liu, A.K. Powell, S. Gao, *Dalton Trans.* 45 (2016) 4614–4621.
- T.R. Younkin, E.F. Conner, J.I. Henderson, S.K. Friedrich, R.H. Grubbs, D. A. Bansleben, *Science* 287 (2000) 460–462;
 - X.Q. Wu, D.D. Huang, Z.H. Zhou, W.W. Dong, Y.P. Wu, J. Zhao, D.S. Li, Q. C. Zhang, X.H. Bu, *Dalton Trans.* 46 (2017) 2430–2438;
 - L.L. Liu, C.X. Yu, J.M. Du, S.M. Liu, J.S. Cao, L.F. Ma, *Dalton Trans.* 46 (2016) 12352–12361;
 - L.L. Liu, C.X. Yu, F.J. Ma, Y.R. Li, J.J. Han, L. Lin, L.F. Ma, *Dalton Trans.* 44 (2015) 1636–1645;
 - F.N. Dai, W.D. Fan, J.H. Bi, P. Jiang, D.D. Liu, X.R. Zhang, H. Lin, C.F. Gong, R. M. Wang, L.L. Zhang, D.F. Sun, *Dalton Trans.* 45 (2016) 61–65;
 - X.B. Liu, H. Lin, Z.Y. Xiao, W.D. Fan, A. Huang, R.M. Wang, L.L. Zhang, D. F. Sun, *Dalton Trans.* 45 (2016) 3743–3749.
- J.-W. Cui, S.-X. Hou, Y.-H. Li, G.-H. Cui, *Dalton Trans.* 46 (2017) 16911–16924.
- X. Zhang, X.L. Meng, C.M. Huang, G.H. Cui, *J. Mol. Struct.* 1100 (2015) 94–99;
 - J. Wu, H. Zhang, S. Du, *J. Mater. Chem. C* 4 (2016) 3364–3376;
 - H.Y. Lin, J. Luan, X.L. Wang, J.W. Zhang, G.C. Liu, A.X. Tian, *RSC Adv.* 4 (2014) 62430–62445;
 - Y.J. Yang, M.J. Wang, K.L. Zhang, *J. Mater. Chem. C* 4 (2016) 11404–11418.
- C. Chen, D. Huang, X. Zhang, F. Chen, H. Zhu, Q. Liu, C. Zhang, D. Liao, L. Li, L. Sun, *Inorg. Chem.* 42 (2003) 3540–3548;
 - Y. Aono, H. Yoshida, K. Katoh, B.K. Breedlove, K. Kagesawa, M. Yamashita, *Inorg. Chem.* 54 (2015) 7096–7102;
 - A. Paul, A. Figuerola, V. Bertolasi, S.C. Manna, *Polyhedron* 119 (2016) 460–470;
 - S. Mistri, A. Patra, M.K. Santra, D. Paul, E. Zangrando, H. Puschmann, S. C. Manna, *Chem. Select.* 3 (2018) 9102–9112;
 - A. Bhunia, S. Mistri, R.K. Manne, M.K. Santra, S.C. Manna, *Inorg. Chim. Acta* 491 (2019) 25–33;
 - A. Bhunia, P. Vojtisek, V. Bertolasi, S.C. Manna, *J. Mol. Struct.* 1189 (2019) 94–101;
 - S. Manna, E. Zangrando, H. Puschmann, S.C. Manna, *Polyhedron* 162 (2019) 285–292;
 - S.C. Manna, A. Paul, E. Zangrando, A. Figuerola, *J. Solid State Chem.* 271 (2019) 378–385;
 - S. Manna, E. Zangrando, S.C. Manna, *Polyhedron* 177 (2020), 114296;
 - A. Paul, S. Mistri, V. Bertolasi, S.C. Manna, *Inorg. Chim. Acta* 495 (2019), 119005;
 - S.C. Manna, S. Mistri, A. Patra, M.K. Mahish, D. Saren, R.K. Manne, M.K. Santra, E. Zangrando, H. Puschmann, *Polyhedron* 171 (2019) 77–85.
- Y. Lan, D.K. Kennepohl, B. Moubarak, K.S. Murray, J.D. Cashion, G. B. Jameson, S. Brooker, *Chem. Eur. J.* 9 (2003) 3772–3784;
 - D. Rambabu, C.P. Pooja, A. Pradeep, J. Dhir, *Mater. Chem. A* 2 (2014) 8628–8631;
 - C.A. Bauer, T.V. Timofeeva, T.B. Settersten, B.D. Patterson, V.H. Liu, B. A. Simmons, M.D. Allendorf, *J. Am. Chem. Soc.* 129 (2007) 7136–7144;
 - Z. Shao, C. Huang, X. Han, H. Wang, A. Li, Y. Han, K. Li, H. Hou, Y. Fan, *Dalton Trans.* 44 (2015) 12832–12838.
- T. Wen, D.X. Zhang, J. Zhang, *Inorg. Chem.* 52 (2013) 12–14;
 - Y.-L. Hou, R.W.Y. Sun, X.P. Zhou, J.H. Wang, D. Li, *Chem. Commun.* 50 (2014) 2295–2297;
 - D.P. Jiang, R.X. Yao, F. Ji, X.M. Zhang, *Eur. J. Inorg. Chem.* 4 (2013) 556–562;
 - T.-P. Hu, Y.-Q. Zhao, Z. Jagličić, K. Yu, X.-P. Wang, D. Sun, *Inorg. Chem.* 54 (2015) 7415–7423;
 - X.-P. Wang, Y.-Q. Zhao, Z. Jagličić, S.-N. Wang, S.-J. Lin, X.-Y. Lia, D. Sun, *Dalton Trans.* 44 (2015) 11013–11020.
- J. Lv, J.X. Lin, X.L. Zhao, R. Cao, *Chem. Commun.* 48 (2012) 669–671;
 - B. Liu, Z.T. Yu, J. Yang, H. Wu, Y.Y. Liu, J.F. Ma, *Inorg. Chem.* 50 (2011) 8967–8972;
 - D. Sun, W. Liu, Y. Fu, Z. Fang, F. Sun, X. Fu, Y. Zhang, Z. Li, *Chem. Eur. J.* 20 (2014) 4780–4788.
- S.S. Martínez, E.V. Uribe, *Ultrason. Sonochem.* 19 (2012) 174–178;
 - L. Alamo-Nole, S. Bailon-Ruiz, T. Luna-Pineda, O. Perales-Perezab, F.

- R. Romana, J. Mater. Chem. A 1 (2013) 5509–5516;
c) H.R. Pouretdal, A. Norozi, M.H. Keshavarz, A. Semnani, J. Hazard. Mater. 162 (2009) 674–681.
- [13] a) N. Hussain, V.K. Bhardwaj, Dalton Trans. 45 (2016) 7697–7707;
b) A. Dey, S. Midya, R. Jana, M. Das, J. Datta, A. Layek, P.P. Ray, J. Mater. Sci. Mater. Electron. 27 (2016) 6325.
- [14] a) S.S. Ma, J.J. Xue, Y.M. Zhou, Z.W. Zhang, J. Mater. Chem. A 2 (2014) 7272–7280;
b) R.S. Patil, M.R. Kokate, D.V. Shinde, S.S. Kolekar, S.H. Han, Spectrochim. Acta, Part A 12 (2014) 113–117;
c) M. Andersson, H. Birkedal, N.R. Franklin, T. Ostomel, S. Boettcher, A. E. Palmqvist, G.D. Stucky, Chem. Mater. 17 (2005) 1409–1415;
d) X.T. Hong, Z.P. Wang, W.M. Cai, F. Lu, J. Zhang, Y.Z. Yang, N. Ma, Y.J. Liu, Chem. Mater. 17 (2005) 1548–1552.
- [15] a) Y. Xu, M.A.A. Schoonen, Am. Mineral. 85 (2000) 543–556;
b) H. Gülce, V. Eskizeybek, B. Haspulat, F. Sar, A. Gülce, A. Avc, Ind. Eng. Chem. Res. 52 (2013) 10924–10934.
- [16] L. Liu, D. Wu, B. Zhao, X. Han, J. Wu, H. Hou, Y. Fana, Dalton Trans. 44 (2015) 1406–1411.
- [17] D.D. Perrin, W.L.F. Armarego, D.R. Perrin, Purification of Laboratory Chemicals, Pergamon Press, Oxford, U.K., 1980.
- [18] Nonius (1998). COLLECT. Nonius BV, Delft, The Netherlands.
- [19] Z. Otwinowski, W. Minor, Methods in Enzymology, in: C.W. Carter, R.M. Sweet (Eds.), 276, Macromolecular Crystallography, Academic Press, New York, 1997, pp. 307–326.
- [20] A. Altomare, M.C. Burla, M. Camalli, G.L. Casciarano, C. Giacovazzo, A. Guagliardi, A.G.G. Moliterni, G. Polidori, R. Spagna, J. Appl. Cryst. 32 (1999) 115–119.
- [21] G.M. Sheldrick, Acta Crystallogr. A 64 (2008) 112–122.
- [22] L.J. Farrugia, J. Appl. Crystallogr. 45 (2012) 849–854.
- [23] a) M. Saranya, R. Ramachandran, P. Kollu, S.K. Jeong, A.N. Grace, RSC Adv. 5 (2015) 15831–15837;
b) M. Zhang, L. Wang, T. Zeng, Q. Shang, H. Zhou, Z. Pana, Q. Cheng, Dalton Trans. 47 (2018) 4251–4258;
c) S. Tsunekawa, T. Fukuda, A. Kasuya, J. Appl. Phys. 87 (2000) 1318–1321;
d) A.L. Linsebigler, G.Q. Lu, J.T. Yates, Chem. Rev. 95 (1995) 735–758.
- [24] a) K. Das, A. Datta, S. Roy, J.K. Clegg, E. Garribba, C. Sinha, H. Kara, Polyhedron 78 (2014) 62–71;
b) A.M. Kirillov, Y.Y. Karabach, M. Haukka, M.F.C. Guedes da Silva, J. Sanchiz, M. N. Kopylovich, A.J.L. Pombeiro, Inorg. Chem. 47 (2008) 162–175.
- [25] a) T. Tsumura, N. Kojitan, I. Izumi, N. Iwashita, M. Toyoda, M. J. Inagaki, Mater. Chem. 12 (2002) 1391–1396; b) D. S. Muggli, L. Ding, M. J. Odland, Catal. Lett. 78 (2002) 23–31; c) R. Asahi, T. Morikawa, T. Ohwaki, K. Aoki, Y. Taga, Science 293 (2001) 269–271; d) H. Lin, P. A. Maggard, Cryst. Growth Des. 10 (2010) 1323–1326.
- [26] a) G.H. Cui, C.H. He, C.H. Jiao, J.C. Geng, V.A. Blatov, Cryst. Eng. Comm. 14 (2012) 4210–4216;
b) B. Ahmed, E. Limem, A. Abdel-Wahab, B. Nasr, Ind. Eng. Chem. Res. 50 (2011) 6673–6680;
c) A. Corma, H. Garcia, F.X.L. Xamena, Chem. Rev. 110 (2010) 4606–4655.
- [27] a) C. Galindo, P. Jacques, A. Kalt, J. Photochem. Photobiol. A 130 (2000) 35–47;
b) J. Joseph, H. Destailats, H. Hung, M. Hoffmann, J. Phys. Chem. A 104 (2000) 301–307.
- [28] a) L. Wen, J. Zhao, K. Lv, Y. Wu, K. Deng, X. Leng, D. Li, Cryst. Growth Des. 12 (2012) 1603–1612;
b) J.G. Yu, W.G. Wang, B. Cheng, B.L. Su, J. Phys. Chem. C 113 (2009) 6743–6750;
c) K. Ishibashi, A. Fujishima, T. Watanabe, K. Hashimoto, Electrochem. Commun. 2 (2000) 207–210.